Proceedings of International Computer Symposium 1994
December 12-15, NCTU, Hsinchu, Taiwan, R.O.C.

Suppression of Moiré Patterns in Scanned Halftone Images by Double Scans with Moving Grids[1]

Ching-Yu Yang(楊靖宇) and Wen-Hsiang Tsai[2](蔡文祥)

Department of Computer and Information Science
National Chiao Tung University
Hsinchu, Taiwan 300
Republic of China

Abstract

Moiré patterns often appear in the image obtained from scanning a printing on a magazine or a newspaper. The patterns do not exist in the original printing but come from alias sampling of screened halftone pictures. A new method of scanning is proposed to suppress the moiré patterns. First, the Fourier analyses of both screening and scanning are presented, from which the new moiré suppression scanning method is derived. The method employs a double-scan process. In the second scan, we shift the scanning position by half of the sampling grid distance of the first scan. Then by averaging the images of the two scans, most of the moiré fringes can be removed. Some experimental results are shown to prove the feasibility of the proposed approach.

1. Introduction

Most printed articles are produced by the planographic printing technique, in which only a few color inks are used. By this technique, we can hardly print images using as many color inks as in the source images. For example, a common gray-scale image contains 256 gray levels. It is impossible to produce a printing using corresponding 256 gray inks. It is necessary to perform a screening process to translate a gray-scale image into a halftone image. A halftone image is a high-frequency black and white image, in which gray intensities are represented as black dots of different sizes. The black dots in a halftone image are spread periodically and orthogonally in order to comfort the human eyes. Practically, a software or machine, called raster image processor (RIP), is required to generate halftone images. The generated halftone image can then be printed by the planographic technique.

1 This work was supported by National Science Council, Republic of China under grant NSC83-0408-E009-010.

2 To whom all correspondence should be sent.

When we scan an image with periodic structures, aliasing is unavoidable and additional moiré patterns will usually appear in the scanning result [1]. Because screen dots repeat periodically in a halftone image, scanning a halftone image will generate additional moiré patterns. Fourier analysis can be employed to describe this phenomenon. In this paper, the Fourier analyses of both the screening and the scanning processes will be presented.

According to the structure of scanner hardware, the process of image scanning can be divided into three major stages. The first stage is pre-filtering which is an optical process related to the characteristic of the scanner lens. For a large drum scanner, a user can adjust the focus and aperture of the lens to make the scanning result sharper or smoother. The next stage is the sampling process which is realized by motor moving or CCD arrangement. A user can adjust the scanning resolution to change sampling grids. Brightness of the scanned picture will also be quantized into digital values. The final stage is post-filtering which is a software process employed to correct digital image values by gamma correction, look up tables (LUT), or other software filters.

Fig. 1 shows a flowchart of the screening and scanning processes. The moiré phenomenon mainly comes from the thresolding step in screening and the sampling step in scanning. Some works proposed to suppress the moiré patterns are reviewed in the following.

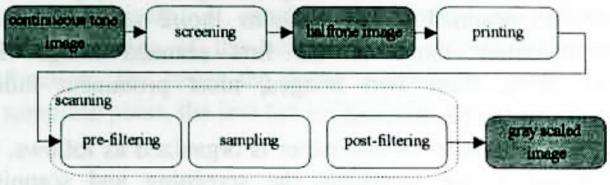

Fig. 1. The screening and scanning flow.

(1) Smoothing is a natural way to remove high-frequency noise. A scanner operator usually adjusts the focus or aperture in the pre-filtering stage to smooth the scanning result in order to suppress the moiré

phenomenon. As is well known, smoothing is a low-pass filter in the frequency domain. It removes high-frequency signals from the image. A common image usually has less power in the high-frequency range than in the low-frequency range. Low-pass filtering will reduce the high-frequency halftone screen signals, remove most periodic structures of the image, and make the sampling yield less alias. On the other hand, there are some problems which are related to smoothing. First, the image will be blurred. Next, it is difficult to perform good aperture or focus adjustment. Besides, only high-end drum scanners support these kinds of adjustments in the pre-filtering stage.

(2) Using inverse halftoning as a post-filter is possible. First, all the detail of the halftone image is scanned with higher resolution. By analysis of each screen dot, it is possible to derive a corresponding gray-scale image. Miceli and Parker [2] and Fan [3] proposed algorithms to do this. Some drawbacks of these methods are that the additional processing time may be long and that high-resolution scanning takes longer time and larger memory space.

(3) Shu and Yeh [4] analyzed possible factors that may cause moiré patterns. They figured out a rule to formulate the relationship between scanning resolution, screening resolution, their angles, and moiré visibility. A suggestion to select a scanning resolution was proposed to make scanning yield minimum visibility of moiré patterns.

(4) Russ [5] proposed filtering of images in the frequency domain. Periodic information in the frequency domain is removed by manual masking operations. However, it is difficult to determine in the frequency domain where is the information that causes moiré patterns in the original image.

Most of the above methods are based on single scanning results. In fact, additional scans of different configurations are also helpful to provide information for moiré suppression. A new method is proposed in this paper that employs a double-scan process and yields good suppression of moiré patterns. An additional scan process is introduced that shifts the scanning position by half of the distance between two neighboring scanning grids. The second scanned image contains moiré patterns which complement those of the first scanned image. By averaging these two images, most prominent moiré patterns can be removed.

The remainder of this paper is organized as follows. In Section 2, we formulate the screening and scanning processes. By Fourier analysis, we point out the reason why moiré patterns are generated during halftone image scanning. In Section 3, we describe the proposed moiré suppression scanning method using moving grids. In Section 4, some experimental results are shown, followed by conclusions in Section 5.

2. Fourier analysis of moiré phenomenon

2.1 Fourier analysis of screening

Halftoning is a thresholding process that converts a gray-scale image $g(\vec{r})$ into a binary image $h(\vec{r})$. Thresholding is performed using a thresholding function $s(\vec{r})$. The corresponding binary image value should be 0 (black) if the intensity value of a pixel in the original gray-scale image is less than or equal to that of the thresholding function; on the other hand, it should be 1 (white) if the intensity value is larger than that of the thresolding function, as described in the following:

$$h(\vec{r}) = \begin{cases} 0, g(\vec{r}) \le s(\vec{r}); \\ 1, g(\vec{r}) > s(\vec{r}). \end{cases} \quad (1)$$

According to the fact that the screen dots are spread uniformly and orthogonally, the thresholding function $s(\vec{r})$ can be defined as a convolution of a screen dot function $s_d(\vec{r})$ with a screen lattice:

$$s(\vec{r}) = s_d(\vec{r}) * \sum_{m=-\infty}^{\infty} \sum_{n=-\infty}^{\infty} \delta(\vec{r} - m\vec{r}_1 - n\vec{r}_2) \quad (2)$$

where $\vec{r}_1$ and $\vec{r}_2$ are orthogonal basis vectors of the screen grids which are defined as a combination of $m\vec{r}_1$ and $n\vec{r}_2$ where m and n are integer numbers. Screen dot function $s_d(\vec{r})$ defines how the screen dots extend. In practice, an RIP uses a matrix as the screen dot function. Fig. 2(a) shows a sample matrix with dimension 8 by 8. It can be used to define 64 screen dots of different sizes and shapes. Two examples of the screen dots are shown in Figs. 2(b) and (c). These dots are used to represent 64 different gray intensity values. The thresholding function can be obtained by performing a rotation of the matrix to the direction parallel to $\vec{r}_1$ or $\vec{r}_2$; scaling it to the size of $\frac{1}{2}|\vec{r}_1|$ by $\frac{1}{2}|\vec{r}_2|$; and making a convolution with the screen grids. Fig. 3 shows the thresholding function in the spatial domain along the direction $\vec{r}_1$.

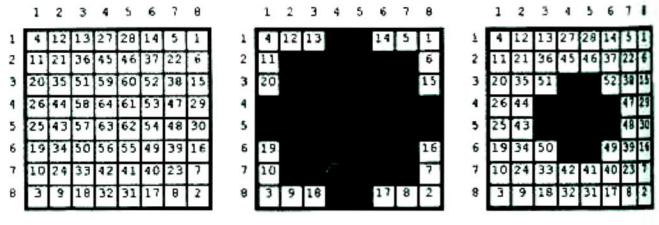

(a) Matrix of screen dot function. (b) Screen dot for gray level 19/64. (c) Screen dot for gray level 53/64.

Fig. 2. Illustration of screen dot function.

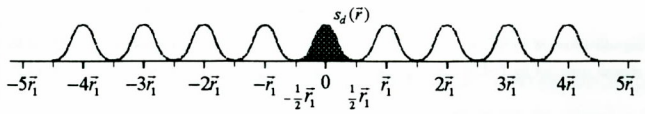

Fig. 3. Thresolding function.

To make the analysis easier, Equation (1) can also be rewritten in the form

$$h(\vec{r}) = \begin{cases} 0, g_n(\vec{r})s(\vec{r}) \le 1; \\ 1, g_n(\vec{r})s(\vec{r}) > 1 \end{cases} \quad (3)$$

where $g_n(\vec{r})$ is the negative function of the original gray-scale image, defined by

$$g_n(\vec{r}) = \frac{1}{g(\vec{r})}.$$

The Fourier transform $H(\vec{w})$ of halftone image $h(\vec{r})$ is related to that of $g_n(\vec{r})s(\vec{r})$ which is:

$$G_n(\vec{w}) * \left[S_d(\vec{w}) \times C_1 \sum_{k=-\infty}^{\infty} \sum_{l=-\infty}^{\infty} \delta(\vec{w} - k\vec{w}_1 - l\vec{w}_2) \right] \quad (4)$$

where $G_n(\vec{w})$ is the Fourier transform of negative gray-scale image $g_n(\vec{r})$; $S_d(\vec{w})$ is the Fourier transform of screen dot function $s_d(\vec{r})$; $\vec{w}_1$ and $\vec{w}_2$ are the reciprocal basis vectors derived from the basis vectors $\vec{r}_1$ and $\vec{r}_2$; and C_1 is a constant.

Fig. 4 shows the relation of the Fourier transforms of the screen dot function, the screen grids, and the thresholding function in the 1-dimensional case. Nonzero values, i. e., the impulses, only occur at frequencies $k\vec{w}_1 + l\vec{w}_2$ where k and l are integer numbers. The convolution of $G_n(\vec{w})$ with the impulses in Fig. 4 results in a function described by (4) and shown in Fig. 5. Because the negative gray-scale image $g_n(\vec{r})$ normally does not vibrate a lot, its Fourier transform $G_n(\vec{w})$ should be a hill function that has less power in the high-frequency range than in the low-frequency range. A convolution of it with an impulse signal at $k\vec{w}_1 + l\vec{w}_2$ should produce a signal component at frequency $k\vec{w}_1 + l\vec{w}_2$. We call such a signal component as a (k,l)-ordered screen component in the frequency domain. From the discussion above, we see that the strength of the (k,l)-ordered screen component decreases by frequency, i. e., the larger k and l are, the smaller the signal.

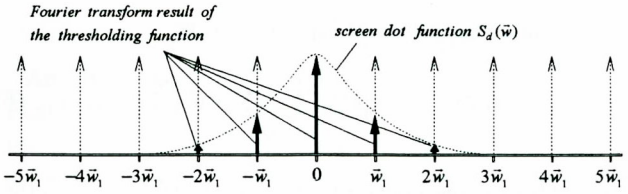

Fig. 4. Relation of Fourier transforms of screen dot function, screen grids, and thresholding function.

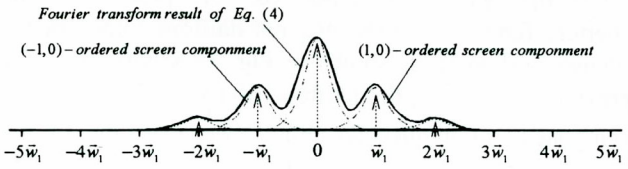

Fig. 5. Fourier transform described by Equation (4).

2.2 Fourier analysis of scanning

As described before, there are three stages in the scanning process. Post-filtering does not affect the moiré fringe. The following equation models the first two stages of scanning, namely, pre-filtering and sampling:

$$g'(\vec{r}) = \left[h(\vec{r}) * a(\vec{r}) \right] \times \sum_{m=-\infty}^{\infty} \sum_{n=-\infty}^{\infty} \delta(\vec{r} - m\vec{\alpha}_1 - n\vec{\alpha}_2) \quad (5)$$

where $\vec{\alpha}_1$ and $\vec{\alpha}_2$ are the basis vectors of the scanning grids; $a(\vec{r})$ is the aperture function which defines the aperture transmittance of the scanner lens; $h(\vec{r})$ is the source halftone image produced by the RIP and printed on paper; and $g'(\vec{r})$ is the gray-scale image resulting from scanning. The first part in Equation (5), the convolution, models the pre-filtering in the scanning process. Light reflected from the printed halftone image is collected by the optics structure of the scanner. After that, light is sampled at position $m\vec{\alpha}_1 + n\vec{\alpha}_2$, where m and n are integers. Fig. 6 shows the aperture function in the spatial domain. It models the focus and aperture characteristics of the scanner lens and is a distance function. The larger the distance from the center of the sampling point, the less the light can be transmitted.

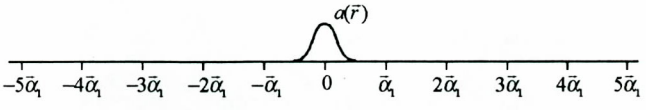

Fig. 6. The aperture function in spatial domain by distance from sampling center.

The Fourier transform of Equation (5) is:

$$G'(\vec{w}) = \left[H(\vec{w}) \times A(\vec{w})\right] * C_2 \sum_{k=-\infty}^{\infty} \sum_{l=-\infty}^{\infty} \delta(\vec{w} - k\vec{u}_1 - l\vec{u}_2) \quad (6)$$

where $H(\vec{w})$ is the Fourier transform of $h(\vec{r})$; $A(\vec{w})$ is the Fourier transform of $a(\vec{r})$; $\vec{u}_1$ and $\vec{u}_2$ are the reciprocal basis vectors derived from $\vec{\alpha}_1$ and $\vec{\alpha}_2$; and C_2 is a constant.

The first part of Equation (6), the product of the aperture function and the original halftone image in the frequency domain, is shown in Fig. 7. According to the previous discussion, the halftone image $H(\vec{w})$ has signal components at frequencies $m\vec{w}_1 + n\vec{w}_2$, i. e., the (m,n)-ordered screen components. The product $H(\vec{w}) \times A(\vec{w})$ should also have the corresponding signal components at $m\vec{w}_1 + n\vec{w}_2$. Then, the product is convolved with the lattices spread by basis vectors $\vec{u}_1$ and $\vec{u}_2$. By the convolution, the signal component of $H(\vec{w}) \times A(\vec{w})$ centered at $m\vec{w}_1 + n\vec{w}_2$ are duplicated at each point of the scanning grids. When $\vec{w}_1$ and $\vec{w}_2$ do not match $\vec{u}_1$ and $\vec{u}_2$, respectively, aliasing occurs. To formulate the phenomenon, we define $m\vec{w}_1 + n\vec{w}_2 = (k \pm a)\vec{u}_1 + (l \pm b)\vec{u}_2$ where m, n, k, and l are integer numbers, and a and b are numbers smaller than 1/2. Then, the (m,n)-ordered screen component will be introduced at frequencies $\pm a\vec{u}_1 \pm b\vec{u}_2$. When a and b are small, the signal component will be placed in the low-frequency area and introduce additional moiré patterns. Such additional signals in the low-frequency area come from the convolution of $H(\vec{w}) \times A(\vec{w})$ with $\delta(\vec{w} - k\vec{u}_1 - l\vec{u}_2)$. We call such signals as (m,n)-ordered moiré signals oriented by (k,l). Fig. 8 illustrates the phenomenon along the $\vec{u}_1$ direction. It is pointed out here that it is the $(\pm 1,0)$-ordered moiré signals oriented by $(\pm 1,0)$ placed in the low-frequency area that introduces the most prominent moiré patterns.

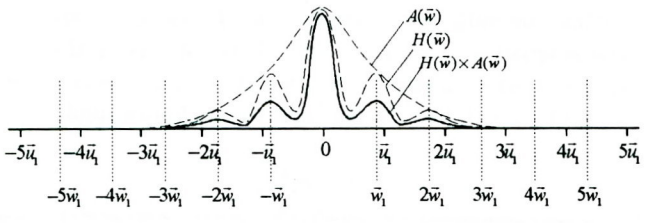

Fig. 7. $H(\vec{w}) \times A(\vec{w})$ in frequency domain.

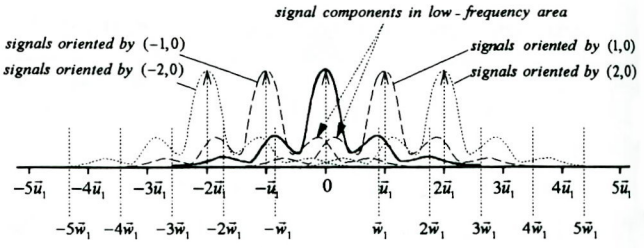

Fig. 8. Signal component at $m\vec{w}_1$ is shifted into the low-frequency area.

3. Proposed double scans with moving grids

Moiré patterns will become very different if we move the sampling grids. By the following analysis, it will be proved that if we move the sampling grids half of the grid distance and rescan the image, the resulting moiré fringes will be negative. Darker moiré patterns will become lighter, and lighter moiré patterns become darker. By averaging the original and the rescanned images, a better image with less moiré phenomenon can be obtained. This is the basic idea of the proposed approach.

First, the effect of the shifting the scanning grids in the frequency domain is checked. The grids in Equation (5) can be modified into the following form to shift the grids half of the grid distance:

$$\sum_{m=-\infty}^{\infty} \sum_{n=-\infty}^{\infty} \delta[\vec{r} - (m + \tfrac{1}{2})\vec{\alpha}_1 - (n + \tfrac{1}{2})\vec{\alpha}_2]. \quad (7)$$

Rewrite Equation (7) as

$$\sum_{m=-\infty}^{\infty} \sum_{n=-\infty}^{\infty} \delta(\vec{r} - \tfrac{1}{2}m\vec{\alpha}_1 - \tfrac{1}{2}n\vec{\alpha}_2) - \sum_{m=-\infty}^{\infty} \sum_{n=-\infty}^{\infty} \delta(\vec{r} - m\vec{\alpha}_1 - n\vec{\alpha}_2), \quad (8)$$

and its Fourier transform becomes

$$2C_2 \sum_{k=-\infty}^{\infty} \sum_{l=-\infty}^{\infty} \delta(\vec{w} - 2k\vec{u}_1 - 2l\vec{u}_2) - C_2 \sum_{k=-\infty}^{\infty} \sum_{l=-\infty}^{\infty} \delta(\vec{w} - k\vec{u}_1 - l\vec{u}_2). \quad (9)$$

For this case, Equation (6) should be modified accordingly as

$$G'(\vec{w}) = \left[H(\vec{w}) \times A(\vec{w})\right] * \left[2C_2 \sum_{k=-\infty}^{\infty} \sum_{l=-\infty}^{\infty} \delta(\vec{w} - 2k\vec{u}_1 - 2l\vec{u}_2) - C_2 \sum_{k=-\infty}^{\infty} \sum_{l=-\infty}^{\infty} \delta(\vec{w} - k\vec{u}_1 - l\vec{u}_2)\right]. \quad (10)$$

Fig. 9 shows that the two peaks of $H(\vec{w})\times A(\vec{w})$ at position $\pm\vec{u}_1$ are complementary to the corresponding ones (i.e., identical in amplitude but different in sign) of $H(\vec{w})\times A(\vec{w})$ in Figure-8. We can also notice that in the low-frequency area, the $(\pm1,0)$-ordered moiré signals oriented by $(\pm1,0)$ are also negative with respect to the corresponding ones in Fig. 8.

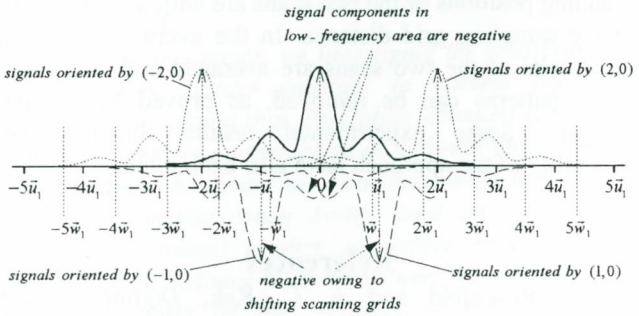

Fig. 9. Result of second scan with half grid distance shift.

We now average the results of the two scans. According to Equation (6) and (10), the signals in the frequency domain become

$$G'(\vec{w})=\left[H(\vec{w})\times A(\vec{w})\right]*C_2\sum_{k=-\infty}^{\infty}\sum_{l=-\infty}^{\infty}\delta(\vec{w}-2k\vec{u}_1-2l\vec{u}_2)\cdot \qquad (11)$$

The averaged signals and the signals removed by the averaging are shown in Fig. 10. Notice that in the low-frequency area, the $(\pm1,0)$-ordered moiré signals oriented by $(\pm1,0)$ have already been removed. The remaining higher-ordered moiré signal components which are placed in the low-frequency area have much smaller amplitudes, and so much less influence on the moiré phenomenon. This means that the major moiré patterns indeed can be removed by double scans with moving grids.

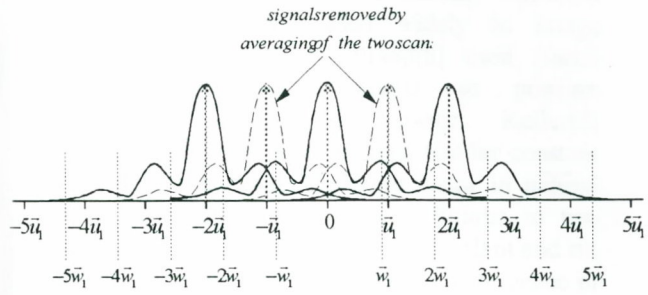

Fig. 10. The averaged signals (shown by solid curves) and the signals removed by the averaging (shown by dashed curves).

4. Experimental results

An image used in the experiment is shown in Fig. 11. First, we print the image by Howteck RIP with 2000 dpi using a 133 lpi screen. Second, we scan the printing with a Howteck D4000 drum scanner using 250 dpi and a balanced aperture. The resulting gray-scale image is shown in Fig. 12 which is full of obvious moiré patterns. Then, we rescan the same printing by shifting the scanning position 0.002 inch horizontally and 0.002 inch vertically. The resulting image with shifted grids is shown in Fig. 13. Moiré patterns again can be seen obvious.

Fig. 14 shows the difference of the images of the two scans, which shows the patterns removed by averaging the two images. The averaged image is shown in Fig. 15. Compared with the result of the first scan, we see that most of the moiré fringes are suppressed.

Fig. 11. Original image.

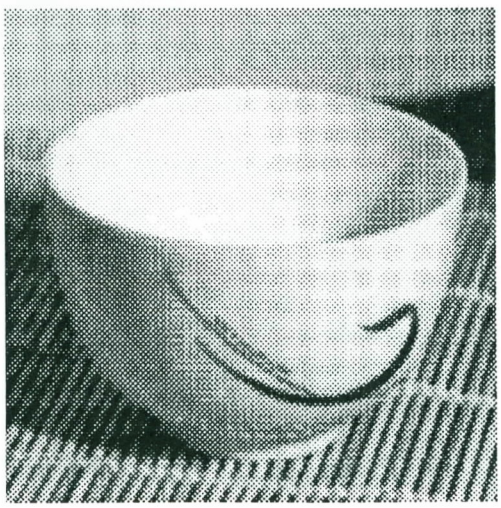

Fig. 12. Result of first scan.

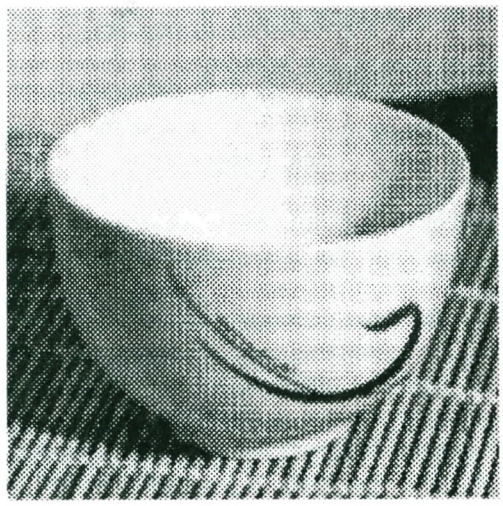

Fig. 13. Result of second scan.

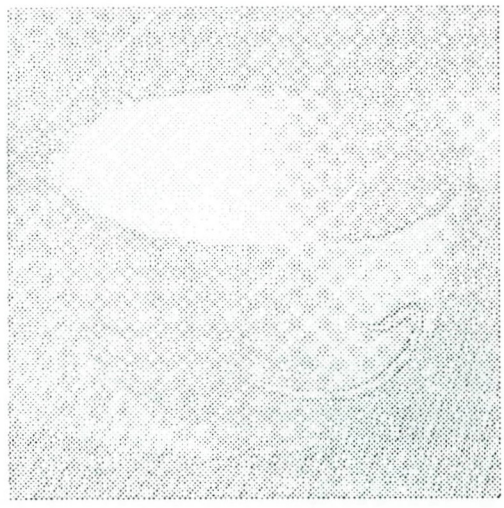

Fig. 14. Difference between the first and the second scans.

Fig. 15. Averaged image from the first and the second scans.

5. Conclusions

When scanning a halftone printing, additional moiré patterns will appear in the scanning result. By Fourier analysis, we have shown that these patterns come from the alias sampling of the screened halftone printing by a scanner. A method which employs a double-scan process, followed by an averaging process, was proposed to suppress the additional moiré patterns. In the double-scan process, we scan the halftone printing twice. The scanning positions of the two scans are with a shift of half of the sampling grid distance. In the averaging process, the results of the two scans are averaged and the major moiré patterns can be removed, as proved by Fourier analysis. Some experimental results showing the feasibility of the approach have also been included.

References

[1] A. Rosenfeld and A. C. Kak, *Digital Picture Processing, 2nd Ed.*, Vol. 1, Academic Press, NY. U. S. A., 1982.

[2] C. M. Miceli and K. J. Parker, "Inverse halftoning," *Journal of Electronic Imaging*, Vol. 1, No. 2, April 1992, pp.143-151.

[3] Zhigang Fan, "Retrieval of gray images from digital halftones," *IEEE International Symposium on Circuits and Systems*, 1992, pp. 2477-2480.

[4] S. P. Shu and C. L. Yeh, "Moiré factors and visibility in scanned and printed halftone images," *Optical Engineering*, Vol. 28, No. 7, July 1989, pp. 805-812.

[5] John C. Russ, *The IMAGE PROCESSING Handbook*, CRC Press, Boca Raton, 1993.